Published in final edited form as:
Org Biomol Chem. 2010 May 7; 8(9): 2028–2036. doi:10.1039/b923465a.

Invader LNA – Efficient Targeting of Short Double Stranded DNA†

Sujay P. Sau[a], **T. Santhosh Kumar**[b], and **Patrick J. Hrdlicka**[a,*]

[a]Department of Chemistry, University of Idaho, Moscow, ID 83844-2343, USA

[b]Nucleic Acid Center, † Department of Physics and Chemistry, University of Southern Denmark, DK-5230 Odense M, Denmark

Abstract

Despite progress with triplex-forming oligonucleotides or helix-invading peptide nucleic acids (PNAs), there remains a need for probes facilitating sequence-unrestricted targeting of double stranded DNA (dsDNA) at physiologically relevant conditions. *Invader LNA* probes, i.e., DNA duplexes with "+1 interstrand zipper arrangements" of intercalator-functionalized 2'-amino-α-L-LNA monomers, are demonstrated herein to recognize short mixed sequence dsDNA targets. This approach, like pseudo-complementary PNA (pcPNA), relies on relative differences in stability between probe duplexes and the corresponding probe:target duplexes for generation of a favourable thermodynamic gradient. Unlike pcPNA, Invader LNA probes take advantage of the "nearest neighbour exclusion principle", i.e., intercalating units of Invader LNA monomers are poorly accommodated in probe duplexes but extraordinarily well tolerated in probe-target duplexes (ΔT_m/modification up to +11.5 °C). Recognition of isosequential dsDNA-targets occurs: a) at experimental temperatures much lower than the thermal denaturation temperatures (T_m's) of Invader LNAs or dsDNA-targets, b) at a wide range of ionic strengths, and c) with good mismatch discrimination. dsDNA recognition is monitored in real-time using inherent pyrene-pyrene excimer signals of Invader LNA probes, which provides insights into reaction kinetics and enables rational design of probes. These properties render Invader LNAs as promising probes for biomedical applications entailing sequence-unrestricted recognition of dsDNA.

INTRODUCTION

Extensive efforts have been made in the past two decades to develop agents for site-specific targeting of double stranded DNA (dsDNA). These efforts have been stimulated by the prospect of developing enabling tools for functional genomics, and discovering novel classes of therapeutic and diagnostic agents[1]. dsDNA-targeting agents have been used in a variety of applications including site-specific modulation of gene expression2،3, induction

†Electronic Supplementary Information (ESI) available: MALDI-MS of 2'-*N*-(pyren-1-yl)methyl-2'-amino-α-L-LNA **ON3**–**ON16** (Table S1), representative thermal denaturation profiles (Fig. S1), hybridization data for **ON3**–**ON16** vs complementary DNA and for Invader LNA probes at different ionic strengths (Tables S2–S5), ΔG^{293}_{rec} for recognition of **ON1**:**ON2** by Invader LNA probes at different ionic strengths (Table S6), additional discussion of thermodynamic parameters, hybridization data for **ON3**–**ON16** vs RNA complements (Table S7), hybridization data for duplexes with various interstrand zipper arrangements of **X** monomers (Table S8), steady-state fluorescence emission spectra of representative Invader LNA probes and probe-target duplexes (Fig. S2), signal decay profile during recognition of dsDNA by representative Invader LNA probes (Fig. S3), steady-state fluorescence emission spectra of duplexes between **ON4** or **ON8** and mismatched DNA targets (Fig. S4), hybridization data for duplexes between **ON1** or **ON2** and mismatched DNA targets (Table S9). See DOI: 10.1039/b000000x/

Corresponding author (PJH); Fax: (+1) 208 885 6173, hrdlicka@uidaho.edu.

†A research center funded by the Danish National Research Foundation for studies on nucleic acid chemical biology.

of site-specific mutagenesis, recombination or repair of genomic DNA[2,3], and direct detection of dsDNA in living cells[4]. Triplex forming oligonucleotides (TFOs)[1–3] and peptide nucleic acids (PNAs)[5,6] are the most widely used dsDNA-targeting probes despite:

- the necessity for long homopurine tracts (>15 nt) in dsDNA targets to ensure sufficient binding affinity/specificity of TFOs/PNAs[1],
- weak pH-dependent Hoogsteen base pairs between TC-motif TFOs and dsDNA, although this has been addressed by modification of TFOs with affinity-enhancing building blocks such as 2'-deoxy-5-methylcytidine, C5-functionalized pyrimidines[7–9], Locked Nucleic Acid (LNA)[10–12], α-L-LNA[13], Bridged Nucleic Acids (BNAs)[14,15], C5-alkynyl functionalized LNA[16] and non-nucleosidic monomers[17],
- formation of secondary structures by G-rich TFOs in the presence of physiological concentrations of potassium ions, which affects dsDNA target binding[18,19], and
- the need for non-physiological ionic strengths to facilitate strand invasion by PNA[5,6].

Accordingly, there has been an intense search for alternative probe technologies that facilitate recognition of mixed sequence dsDNA targets[20]. Examples include minor groove binding polyamides[21], TFOs capable of recognizing all four Watson-Crick base pairs via the major groove[22,23], optimized PNAs[24,25], antigene (ag) PNA[26,27], agLNA[28,29], "Zorro" LNA[30], pseudo-complementary (pc) DNA[31,32], pcPNA[33–38], and other approaches[39–41]. While these emerging probe strategies are promising, there remains a need for a probe technology that allows fast, efficient and specific dsDNA targeting at physiologically relevant ionic strengths with minimal sequence restrictions and uncomplicated "DNA-like" handling (adequate aqueous solubility, compatibility with delivery agents).

We have recently introduced N2'-intercalator-functionalized 2'-amino-α-L-LNA and have demonstrated their ability to precisely direct the appended intercalators into the core of DNA duplexes[42–47]. As a result, extraordinary increases in thermal affinity toward DNA complements of up to +19.5 °C per modification are observed relative to unmodified reference strands. This has facilitated the development of probes for detection of single nucleotide polymorphisms[45] and stabilization of abasic sites[46].

Herein, we demonstrate recognition of isosequential dsDNA targets using double stranded 2'-*N*-(pyren-1-yl)methyl-2'-amino-α-L-LNA probes dubbed *Invader LNA*[€,42] in buffers of varying ionic strength (Fig. 1). Important insights into the thermodynamics and kinetics of the recognition events are gained from thermal denaturation, steady-state fluorescence and fluorescence decay experiments, allowing the identification of key design principles.

RESULTS AND DISCUSSION

Thermal denaturation properties of 2'-*N*-(pyren-1-yl)methyl-2'-amino-α-L-LNA

Singly modified 2'-*N*-(pyren-1-yl)methyl-2'-amino-α-L-LNA form extraordinarily stable duplexes with DNA complements compared to the corresponding unmodified reference DNA duplex **ON1**:**ON2** (ΔT_m = +9.5 to +11.5 °C and $\Delta\Delta G^{293}$ = −9 to −14 kJ/mol, entries 3–9, Table 1). Slightly less stabilized duplexes are observed when monomer **X** is incorporated close to the 5'-terminus (entry 2, Table 1). The corresponding duplexes with

€*Invader LNA*" are defined as double stranded DNA probes with one or more *+1 interstrand zipper arrangements* of intercalator-modified 2'-amino-α-L-LNA monomers. This particular zipper arrangement is also termed *energetic hotspot*, for simplicity. For a formal definition of the 'zipper' nomenclature see Table S4†.

RNA targets are invariably less stable, but still significantly stabilized (ΔT_m/mod-values between +0.5 and +6.0 °C, Table S7[†]).

ONs modified with two 2'-*N*-(pyren-1-yl)methyl-2'-amino-α-L-LNA **X** monomers positioned as next-nearest neighbours exhibit slightly less-than-additive increases in thermal affinity (compare e.g. entries 2, 3 and 10, Table 1). Conversely, when two **X** monomers in an ON are separated by greater distances, more-than-additive increases in thermal affinity are observed (compare e.g. entries 2, 5 and 12, Table 1), resulting in the formation of highly stabilized duplexes with ΔT_m-values up to +23.5 °C.

The increased thermal affinity of 2'-*N*-(pyren-1-yl)methyl-2'-amino-α-L-LNA **ON3–ON16** toward complementary DNA primarily arises from less unfavourable entropic contributions that either are not fully counterbalanced by less favourable enthalpic contributions (entries 2–5 and 10–11, Table 1) or are augmented by marginally more favourable enthalpic contributions (entries 7–8, 12–13 and 15, Table 1). This most likely reflects the conformational preorganization of the bicyclic 2'-amino-α-L-LNA skeleton, which directs the appended pyrene moiety to the duplex core for favourable intercalation (Fig. 1) [42–47].

Thermal denaturation properties of Invader LNA probes

Double stranded 2'-*N*-(pyren-1-yl)methyl-2'-amino-α-L-LNA probes with a single "+1 interstrand zipper arrangement" of **X** monomers are relatively unstable (ΔT_m = −1.5 to +3.5 °C and $\Delta\Delta G^{293}$ = −3.0 to +9.0 kJ/mol, entries 1–4, Table 2). For the sake of simplicity, *probes with +1 zipper arrangements of **X** monomers are henceforth dubbed "Invader LNA", and these particular zipper arrangements are dubbed "energetic hotspots"*[42,€]. The low stability of Invader LNA probes most likely reflects a violation of the 'nearest neighbour exclusion principle', which states that intercalators at most bind to every second base pair of a DNA duplex due to constraints in the local expandability of duplexes[49]. Invader LNA probes feature one intercalator per base pair (Fig. 1). Two additional observations support this hypothesis. First, the less favourable enthalpy of Invader LNA probes indicates intercalator-mediated perturbation of local duplex geometry and base pairing (see $\Delta\Delta H$ for entries 1–4, Table 2). Secondly, DNA duplexes with other interstrand zipper arrangements of **X** monomers and therefore lower local densities of intercalating units, are extraordinarily stable (ΔT_m = +16.5 °C to +22.0 °C for −3, −1, +3 and +5 zippers, Table S8[†]).

Invader LNA with two *energetic hotspots* form surprisingly stable duplexes (ΔT_m = +10.5 to +15.5 °C, entries 5–7, Table 2). Interestingly, this trend is *not paralleled* in the change in free energy upon hybridization at 293K ($\Delta\Delta G^{293}$ ~ 1–2 kJ/mol relative to unmodified **ON1**:**ON2**, entries 5–7, Table 2). This is a result of extraordinarily favourable entropic contributions rendering ΔG highly temperature dependent (see $\Delta(\Delta T^{293}S)$ for entries 5–7, respectively, Table 2).

Thermodynamic dsDNA-targeting potential of Invader LNA probes

The abovementioned thermal denaturation studies suggest that it is energetically favourable for Invader LNA probes to dissociate and bind to complementary DNA targets (Fig. 1). To

[†]Electronic Supplementary Information (ESI) available: MALDI-MS of 2'-*N*-(pyren-1-yl)methyl-2'-amino-α-L-LNA **ON3**–**ON16** (Table S1), representative thermal denaturation profiles (Fig. S1), hybridization data for **ON3**–**ON16** vs complementary DNA and for Invader LNA probes at different ionic strengths (Tables S2–S5), ΔG^{293}_{rec} for recognition of **ON1**:**ON2** by Invader LNA probes at different ionic strengths (Table S6), additional discussion of thermodynamic parameters, hybridization data for **ON3**–**ON16** vs RNA complements (Table S7), hybridization data for duplexes with various interstrand zipper arrangements of **X** monomers (Table S8), steady-state fluorescence emission spectra of representative Invader LNA probes and probe-target duplexes (Fig. S2), signal decay profile during recognition of dsDNA by representative Invader LNA probes (Fig. S3), steady-state fluorescence emission spectra of duplexes between **ON4** or **ON8** and mismatched DNA targets (Fig. S4), hybridization data for duplexes between **ON1** or **ON2** and mismatched DNA targets (Table S9). See DOI: 10.1039/b000000x/

quantitatively assess the thermodynamic dsDNA-targeting potential of different Invader LNA probe designs, the available free energy for room temperature recognition of isosequential DNA was estimated as $\Delta G^{293}_{rec} = \Delta G^{293}$ (probe strand 1 : target strand 1) + ΔG^{293} (probe strand 2 : target strand 2) - ΔG^{293} (dsDNA target) - ΔG^{293} (Invader LNA probe) (Table 2)[50]. Probes with a single energetic hotspot provide $\Delta G^{293}_{rec} = -19.0$ to -26.0 kJ/mol (entries 1–4, Table 2), while probes with two energetic hotspots exhibit considerably more inherent free energy for dsDNA-recognition ($\Delta G^{293}_{rec} = -34.0$ kJ/mol to -50.0 kJ/mol, entries 5–7, Table 2). Invader LNA probes with two hotspots separated by two or four base pairs exhibit additive increases in ΔG^{293}_{rec}-values relative to the corresponding single hotspot Invader LNA probes (e.g., compare ΔG^{293}_{rec}-values for entries 1, 3 and 6, Table 2). This contrasts Invader LNA probes with sequentially incorporated hotspots. This suggests that Invader LNA probes should feature two separated energetic hotspots for maximized thermodynamic dsDNA-targeting potential.

Fluorescence properties of Invader LNA probes

Steady-state fluorescence emission spectra of *all* Invader LNA probes obtained using an excitation wavelength λ_{ex} = 335 nm, exhibit structured pyrene monomer peaks at λ_{max} = 380 nm and 400 nm along with an intense unstructured peak centered at λ_{max} = 495 nm (Fig. 2 and Fig S2[†]). Duplexes with other interstrand zipper arrangements of **X** monomers only exhibit marginal signal intensity at 495 nm (results not shown). Pyrene emission signals at 495 nm are routinely attributed to pyrene-pyrene excimers[41,42,45,51–55], suggesting that the pyrene moieties of the two **X** monomers comprising the energetic hotspots in Invader LNA probes are separated by ~3.4 Å[56] (Fig. 1). In contrast, emission spectra of duplexes between 2'-*N*-(pyren-1-yl)methyl-2'-amino-α-L-LNA and complementary DNA exhibit pyrene monomer fluorescence and only negligible excimer signals (Fig. 2 for **ON4**:**ON2** and **ON1**:**ON8**; see also Fig. S2[†]). Given these experimental observations, the signal intensity at λ_{em} = 495 nm can accordingly be used as an inherent optical readout to monitor dsDNA recognition by Invader LNA probes in real-time.

Targeting of dsDNA by Invader LNA probes

Pre-annealed Invader LNA probes were added to an equimolar quantity of their *pre-annealed isosequential 13-mer dsDNA target* **ON1**:**ON2** (all strands at 1.0 μM). The recognition experiments were performed in thermal denaturation buffer ($[Na^+]$ = 110 mM, pH 7) at an *experimental temperature (T_{exp} = 20 °C) markedly below the T_m-values* of dsDNA target **ON1**:**ON2** (37.5 °C, Table 1), Invader LNA probes (36–53 °C, Table 2) and the corresponding probe-target duplexes (44.5–61.0 °C, Table 2). Addition of Invader LNA probes results in a rapid decrease in excimer intensity (λ_{em} = 495 nm) as the two stacking pyrene moieties of the probes are forced apart (Fig. 1) during recognition of the dsDNA target (Fig. 3 and Fig S3[†]). The excimer signals decay according to a first order rate equation when equimolar quantities between Invader LNA and dsDNA targets are used, but become more complex when non-equimolar quantities of probes and targets are used (results not shown).

Electrophoretic mobility shift assays (EMSAs, 16 % non-denaturing PAGE) were performed to validate the fluorescence-based assay as a convenient method to monitor dsDNA-recognition by Invader LNA probes. The representative single hotspot Invader LNA **ON4:ON8** exhibits significantly lower electrophoretic mobility than isosequential dsDNA target **ON1**:**ON2** and probe-target duplexes **ON1:ON8** and **ON4:ON2** (Fig. 4). The difference in electrophoretic mobility between the dsDNA target and probe-target duplexes is much smaller although discernible (compare lanes 1, 2, and 4, Fig. 4). We attribute the observed differences to a) an extensively distorted duplex geometry of Invader LNA probe **ON4**:**ON8** as suggested by thermodynamic data (Table 2) and preliminary results from

molecular modelling (results not shown), and b) slightly perturbed probe-target duplex geometry (elongation) upon intercalation of a single pyrene moiety, as previously reported[47].

Incubation of equimolar quantities of Invader LNA **ON4**:**ON8** and dsDNA target **ON1**:**ON2** at room temperature or 37 °C results in disappearance of the bands corresponding to the Invader LNA probe and dsDNA target. Instead, a single band with identical electrophoretic mobility as probe-target duplexes **ON1:ON8** and **ON4:ON2** emerges (compare lanes 6–8 with lanes 1, 2 and 5). Incubation of Invader LNA and dsDNA at 4 °C results in incomplete recognition as indicated by the presence of weak bands corresponding to **ON4**:**ON8** and **ON1**:**ON2**. These observations are in line with the results from the fluorescence assay (Fig. 3) and demonstrate that the decrease in excimer signal intensity upon addition of Invader LNA probes to isosequential dsDNA targets is attributable to dsDNA-recognition.

The time period resulting in a 50% or 75% decrease of the original excimer signal ($t_{50\%}$ or $t_{75\%}$) was determined for four representative Invader LNA to assess recognition kinetics. The selected Invader LNA probes include two single hotspot Invader LNAs (**ON4**:**ON8** and **ON6**:**ON10**), and two double hotspot Invader LNAs where the hotspots are separated by zero or four base pairs (**ON11**:**ON14** and **ON13**:**ON16**, respectively). Recognition of **ON1**:**ON2** occurred quickly at 20 °C with all studied Invader LNA probes ($t_{50\%}$ = 29–48 min, entry 1, Table 3), but was particularly fast with **ON11**:**ON14** having two sequentially positioned hotspots. Interestingly, Invader LNA probe **ON13**:**ON16** exhibits the most favourable ΔG^{293}_{rec}-value for recognition of dsDNA **ON1**:**ON2** (Table 2) and yet displays the slowest recognition kinetics (Table 3). Increases in experimental temperatures result in faster dsDNA-recognition ($t_{50\%}$ = 37.5/29.0, 14.2/11.1, 4.8/4.3, 1.5/1.6 and 0.5/0.6 min at T_{exp} = 20, 22.5, 25, 27.5 and 30 °C for **ON4**:**ON8**/**ON11**:**ON14**, respectively).

Next, the ability of Invader LNA probes to discriminate between correct and incorrect dsDNA targets was evaluated. Addition of representative Invader LNA probe **ON4**:**ON8** to fully base paired but *non-isosequential* dsDNA targets generally resulted in a slower and less pronounced decay of the excimer signal (Fig. 5). More specifically, the signal intensity at 495 nm decreased by 35–45% to reach a plateau ~200 min after addition of **ON4**:**ON8** to 13-mer dsDNA targets containing a single sequence disparity at positions outside the hotspot region (**ON17**:**ON18** or **ON25**:**ON26**, Fig. 5; sequences shown in Table 4). Slower but more pronounced decreases in excimer signal (~70% decrease after >16 h) were observed upon addition of Invader LNA probes **ON4**:**ON8** to 13-mer dsDNA targets **ON21**:**ON22** or **ON23**:**ON24** with single sequence disparities within the hotspot regions. Thus, the data suggest that Invader LNA probes discriminate mismatched dsDNA targets well[$].

In agreement with these observations, unfavourable or marginally favourable ΔG^{293}_{rec}-values are observed for recognition of non-isosequential dsDNA targets by Invader LNA probe **ON4**:**ON8** (Table 4). This reflects the energetic penalty upon hybridization of 2'-*N*-(pyren-1-yl)methyl-2'-amino-α-L-LNA **ON4** or **ON8** to mismatched DNA strands (see $\Delta(\Delta G^{293})$-values, Table 5). **ON4** and **ON8** discriminate DNA strands with mismatches opposite of deoxyribonucleotides well (compare ΔT_m-values of entries 1 and 5–10 in Table 5 and Table S9[†]). In contrast, mismatched DNA targets with thymine or guanine moieties opposite of thymine monomer **X** are less efficiently discriminated (see entries 3–4, Table 5). This translates in marginally favourable ΔG^{293}_{rec}-values for recognition of **ON21**:**ON22** and

[$]For steady-state fluorescence emission spectra of duplexes between **ON4** or **ON8** and mismatched DNA targets and additional discussion, see Fig. S4.

ON23:**ON24** by Invader LNA probe **ON4**:**ON8** (entries 4–5, Table 4) and the distinct signal decay profile during dsDNA recognition (Fig. 5).

Discrimination of non-isosequential dsDNA targets can likely be improved in next-generation Invader LNA probes using recently reported N2'-intercalator-functionalized 2'-amino-α-L-LNA building blocks, which exhibit significantly improved thermal discrimination of mismatched DNA[44,47].

Finally, the influence of buffer composition on dsDNA-recognition by Invader LNA probes was studied. Representative Invader LNA probes **ON4**:**ON8** or **ON11**:**ON14** were added to isosequential dsDNA target **ON1**:**ON2** as described above except for the use of buffers that either represent physiological conditions more accurately (KMST-buffer: pH 7.2, 140 mM KCl, 10 mM $MgCl_2$, 1 mM spermine and 40 mM Tris-Cl) or are of very high ionic strength ($[Na^+]$ = 710 mM). Recognition of dsDNA targets was observed in both buffers at 20 °C, and particularly rapid with Invader LNA probe **ON11**:**ON14** featuring two sequentially incorporated energetic hotspots (Table 3). These observations suggest that Invader LNA probes may be applicable over a significantly wider range of conditions than PNA-based dsDNA-targeting approaches [5,6,33–38].

Interestingly, Invader LNA probe **ON11**:**ON14** has less free energy available for targeting of dsDNA at high salt conditions than **ON4**:**ON8** (see ΔG^{293}_{rec}-values, Table S6†). Thus, a favourable energetic gradient ($\Delta G^{293}_{rec} \ll 0$ kJ/mol) is a prerequisite for successful dsDNA-targeting by Invader LNA probes, but reaction kinetics must be taken into consideration for practical applications. Both aspects strongly depend on by the number and position of energetic hotspots within the probes. Invader LNA probes with two sequentially incorporated energetic hotspots are thermodynamically as well as kinetically activated toward recognition of dsDNA.

The successful targeting of dsDNA target **ON1**:**ON2** with Invade r LNA **ON11**:**ON14** at high salt conditions is remarkable considering that the experimental temperature (T_{exp} = 20 °C) is markedly lower than the thermal denaturation temperatures of the dsDNA target, Invader LNA probe, and probe:target duplexes **ON1**:**ON14** and **ON11**:**ON2** (T_m = 45.5 °C, 59.0 °C, 59.0 °C and 63.5 °C, respectively, Tables S2 and S4†, respectively).

While additional studies will be needed to elucidate the recognition mechanism, the data presented herein seem inconsistent with a dissociative pathway[57]. This pathway would involve dissociation of Invader LNA probes and dsDNA targets into four single strands (which is not likely to occur at $T_{exp} \ll T_m$), followed by energetically favourable self-assembly of probe-target duplexes. We speculate that a *sequential displacement pathway*[57] may be involved where partial melting of dsDNA targets and Invader LNA probes reveals nucleation sites serving as initiation sites for formation of probe-target duplexes. Within this hypothesis, kinetic activation of Invader LNA probes with two sequential hotspots could be related to more efficient formation of nucleation sites.

CONCLUSION AND OUTLOOK

Important features and design principles of Invader LNA probes have been identified during the course of this study:

- The Invader LNA approach is general. Every investigated Invader LNA probe displays fast recognition of isosequential dsDNA targets in a variety of buffers, including buffers mimicking physiological conditions.

- Recognition of mixed sequence dsDNA targets is conveniently followed in real-time by decreases in the pyrenepyrene excimer signal inherently exhibited by Invader LNA probes.
- Invader LNA probes with two sequentially incorporated hotspots exhibit more pronounced thermodynamic gradients and are kinetically more activated toward dsDNA-recognition than single hotspot probes.
- Invader LNA probes discriminate non-isosequential dsDNA targets.

The ability of Invader LNA probes to thermodynamically and kinetically discriminate mismatched dsDNA-targets can be envisioned to result in the development of sensors for detection of single nucleotide polymorphism[58,59]. Moreover, recent reports on the use of Zorro LNA[30] and agLNA[28,29] for recognition of accessible target regions within plasmids or chromosomal DNA, warrant evaluation of optimized Invader LNA probes as site-specific modulators of gene expression[60]. Studies along these lines are currently underway in our laboratory.

Experimental

MATERIALS

Synthesis of 2'-*N*-(pyren-1-yl)methyl-2'-amino-α-L-LNA—The corresponding phosphoramidite of monomer **X** was obtained and incorporated into 13-mer AT-rich oligodeoxyribonucleotides (ONs) using established protocols[42,47]. Briefly described, automated synthesis of ONs was performed in 0.2 μmol scale applying standard procedures except for extended coupling times (30 min, using 1*H*-tetrazole as catalyst), which resulted in stepwise coupling yields of ~99% for monomers **X** (Fig. 1). Following standard workup and purification, the composition and purity (>80%) of modified ONs was verified by MALDI-MS (Table S1[†]) and ion-exchange HPLC, respectively.

Thermal denaturation studies—Concentrations of all ONs were estimated using the following extinction coefficients ($L \times mmol^{-1} \times cm^{-1}$) at 260 nm: dA (15.20), dC (7.05), dG (12.01), T (8.40); rA (15.40), rC (9.00), rG (13.70), rU (10.00); pyrene (22.40). ONs (1.0 μM each strand) were thoroughly mixed in T_m-buffer (see below), denatured by heating and subsequently cooled to the starting temperature of the experiment. Thermal denaturation curves (A_{260} vs. T) were recorded using a Cary 100 UV/VIS spectrometer equipped with a Peltier temperature programmer. The temperature was varied from at least 15 °C below to 15 °C above the thermal denaturation temperature (T_m) using a ramp of 0.5 °C/min. Quartz optical cells with a path length of 10 mm were used. In general, a medium salt T_m-buffer was used (100 mM NaCl, 0.1 mM EDTA, pH 7.0 adjusted with 10 mM NaH_2PO_4/5 mM Na_2HPO_4). Other utilized buffers include low and high salt buffers (composition as for medium salt buffer except that 0 mM and 700 mM NaCl were used, respectively) and a KMST-buffer (140 mM KCl, 10 mM $MgCl_2$, 1 mM spermine and 40 mM Tris-Cl, pH 7.2). Thermal denaturation temperatures and thermodynamic parameters for duplex formation were determined by baseline fitting of melting curves using software provided with the UV/VIS spectrometer. Bimolecular reactions, two-state melting behaviour and a heat capacity change $\Delta C_p = 0$ upon hybridization were assumed[48]. The validity of these assumptions for N2'-functionalized 2'-amino-α-L-LNA have been previously discussed[47]. Reported thermal denaturation temperatures were determined as an average from two separate experiments within ±1.0 °C. For determination of thermodynamic parameters, a minimum of two experimental denaturation curves were each analyzed at least three times to minimize errors arising from baseline choice, and average values are listed. Changes in Gibbs free energy and entropy upon duplex formation were determined at the temperatures of the dsDNA-targeting experiments (T_{exp}= 293.15 K).

Steady-state fluorescence emission experiments—Fluorescence measurements were performed on a Cary Eclipse fluorimeter equipped with a Peltier temperature controller using quartz optical cells with a path length of 10 mm. A concentration of 1.0 μM of each strand in medium salt T_m-buffer was used. No corrections for the minimal solvent background or attempts to eliminate dissolved oxygen from the buffer solution were made. Mixtures were kept at 20 °C (±0.2 °C) at all times. Steady-state fluorescence emission spectra (360–600 nm) were obtained using an excitation wavelength of 335 nm, excitation and emission slits of 5.0 nm and photomultiplier voltage set at 800V. The setup for dsDNA-targeting experiments is detailed in the Results and Discussion section.

Electrophoretic mobility shift assays—Stock solutions (4 μM) of dsDNA targets, Invader LNA probes and probe-target duplexes were prepared by annealing appropriate complementary single strands in a pH 7.2 incubation buffer (70 mM HEPES, 15 mM $MgCl_2$, 15% sucrose, 0.15% spermine, 300 mM NaCl) and storing the solutions at 4°C. Control duplexes (4 μL) or reaction mixtures (4 μL of each duplex) were incubated as described in Figure 5, mixed with 6× DNA loading dye solution (2 μL), loaded onto a 16% native polyacrylamide gel in 1× TBM buffer (89 mM Tris, 89 mM boric acid, 10 mM $MgCl_2$ and run for 24 h at 10 V/cm and 4 °C. Gels were stained with SYBR Gold and documented on a Flour S multiimager.

Supplementary Material

Refer to Web version on PubMed Central for supplementary material.

Acknowledgments

The input of Prof. Jesper Wengel (Nucleic Acid Center, Univ. Southern Denmark) during initial stages of this project is highly appreciated. We thank Dr. Rod Hill and Dr. Madhusudhan Papasani (AVS, Univ. Idaho) for access to and assistance with the Flour S multiimager.

FUNDING

This study was supported by Award Number R01 GM088697 from the National Institute Of General Medical Sciences, National Institutes of Health [grant number P20 RR016448 from the COBRE Program of the National Center for Research Resources]; Idaho NSF EPSCoR; the BANTech Center at Univ. Idaho; a Univ. Idaho Research Office and Research Council Seed Grant; The Danish National Research Foundation; and the Nucleic Acid Based Drug Design Ph.D. school (NAC DRUG; supported by the Danish Agency for Science Technology and Innovation).

References

1. Duca M, Vekhoff P, Oussedik K, Halby L, Arimondo PB. Nucleic Acids Res 2008;36:5123–5138. [PubMed: 18676453]
2. Rogers FA, Lloyd JA, Glazer PM. Curr. Med. Chem. Anti-Cancer Agents 2005;5:319–326.
3. Besch R, Giovannangeli C, Degitz K. Curr. Drug Targets 2004;5:691–703. [PubMed: 15578950]
4. Ghosh I, Stains CI, Ooi AT, Segal DJ. Mol. BioSyst 2006;2:551–560. [PubMed: 17216036]
5. Kaihatsu K, Janowski BA, Corey DR. Chem. Biol 2004;11:749–758. [PubMed: 15217608]
6. Nielsen, PE. Sequence-Specific DNA Binding Agents. Michael, J., editor. Cambridge, UK: Warring, Royal Society of Chemistry; 2006. p. 96-108.
7. Bijapur J, Keppler MD, Bergqvist S, Brown T, Fox KR. Nucleic Acids Res 1999;27:1802–1809. [PubMed: 10101187]
8. Brazier JA, Shibata T, Townsley J, Taylor BF, Frary E, Williams NH, Williams DM. Nucleic Acids Res 2005;33:1362–1371. [PubMed: 15745996]
9. Li H, Miller PS, Seidman MM. Org. Biomol. Chem 2008;6:4212–4217. [PubMed: 18972052]

10. Torigoe H, Hari Y, Sekiguchi M, Obika S, Imanishi T. J. Biol. Chem 2001;276:2354–2360. [PubMed: 11035027]
11. Sun B-W, Babu BR, Sørensen MD, Zakrzewska K, Wengel J, Sun J-S. Biochemistry 2004;43:4160–4169. [PubMed: 15065859]
12. Brunet E, Alberti P, Perrouault L, Babu BR, Wengel J, Giovannangeli C. J. Biol. Chem 2005;280:20076–20085. [PubMed: 15760901]
13. Kumar N, Nielsen KE, Maiti S, Petersen M. J. Am. Chem. Soc 2006;128:14–15. [PubMed: 16390098]
14. Koizumi M, Morita K, Daigo M, Tsutsumi S, Abe K, Obika S, Imanishi T. Nucleic Acids Res 2003;31:3267–3273. [PubMed: 12799454]
15. Rahman SMA, Seki S, Obika S, Yoshikawa H, Miyashita K, Imanishi T. J. Am. Chem. Soc 2008;130:4886–4896. [PubMed: 18341342]
16. Sau SP, Kumar P, Anderson BA, østergaard ME, Deobald L, Paszczynski A, Sharma PK, Hrdlicka PJ. Chem. Commun 2009:6756–6758.
17. Filichev VV, Pedersen EB. J. Am. Chem. Soc 2005;127:14849–14858. [PubMed: 16231939]
18. Cheng A-J, Van Dyke MW. Nucleic Acids Res 1993;21:5630–5635. [PubMed: 8284208]
19. Dagle JM, Weeks DL. Nucleic Acids Res 1996;24:2143–2149. [PubMed: 8668547]
20. Simon P, Cannata F, Concordet J-P, Giovannangeli C. Biochimie 2008;90:1109–1116. [PubMed: 18460344]
21. Dervan PB, Doss RM, Marques MA. Curr. Med. Chem. Anti-cancer Agents 2005;5:373–387.
22. Fox KR, Brown T. Quart. Rev. Biophys 2005;38:311–320.
23. Rusling DA, Powers VEC, Ranasinghe RT, Wang Y, Osborne SD, Brown T, Fox KR. Nucleic Acids Res 2005;33:3025–3032. [PubMed: 15911633]
24. Rapireddy S, He G, Roy S, Armitage BA, Ly DH. J. Am. Chem. Soc 2007;129:15596–15600. [PubMed: 18027941]
25. Chenna V, Rapireddy S, Sahu B, Ausin C, Pedroso E, Ly DH. ChemBioChem 2008;9:2388–2391. [PubMed: 18816545]
26. Janowski BA, Kaihatsu K, Huffman KE, Schwartz JC, Ram R, Hardy D, Mendelson CR, Corey DR. Nat. Chem. Biol 2005;1:210–215. [PubMed: 16408037]
27. Hu J, Corey DR. Biochemistry 2007;46:7581–7589. [PubMed: 17536840]
28. Beane R, Ram R, Gabillet S, Arar K, Monia BP, Corey DR. Biochemistry 2007;46:7572–7580. [PubMed: 17536839]
29. Beane R, Gabillet S, Montaillier C, Arar K, Corey DR. Biochemistry 2008;47:13147–13149. [PubMed: 19053275]
30. Ge R, Heinonen JE, Svahn MG, Mohamed AJ, Lundin KE, Smith CIE. FASEB J 2007;21:1902–1914. [PubMed: 17314142]
31. Kutyavin IV, Rhinehart RL, Lukhtanov EA, Gorn VV, Meyer RB Jr, Gamper HB Jr. Biochemistry 1996;35:11170–11176. [PubMed: 8780521]
32. Woo J, Meyer RB Jr, Gamper HB Jr. Nucleic Acids Res 1996;24:2470–2475. [PubMed: 8692683]
33. Lohse J, Dahl O, Nielsen PE. Proc. Natl. Acad. Sci. U.S.A 1999:11804–11808. [PubMed: 10518531]
34. Izvolsky KI, Demidov VV, Nielsen PE, Frank-Kamenetskii MD. Biochemistry 2000;39:10908–10913. [PubMed: 10978178]
35. Demidov VV, Protozanova E, Izvolsky KI, Price C, Nielsen PE, Frank-Kamenetskii MD. Proc. Natl. Acad. Sci. U.S.A 2002;99:5953–5958. [PubMed: 11972051]
36. Smolina IV, Demidov VV, Soldatenkov VA, Chasovskikh SG, Frank-Kamenetskii MD. Nucleic Acids Res 2005;33:e146. [PubMed: 16204449]
37. Kim K-H, Nielsen PE, Glazer PM. Nucleic Acids Res 2007;35:7604–7613. [PubMed: 17977869]
38. Ishizuka T, Yoshida J, Yamamoto Y, Sumaoka J, Tedeschi T, Corradini R, Sforza S, Komiyama M. Nucleic Acids Res 2008;36:1464–1471. [PubMed: 18203747]
39. Bryld T, Højland T, Wengel J. Chem. Commun 2004:1064–1065.

40. Filichev VV, Christensen UB, Pedersen EB, Babu BR, Wengel J. ChemBioChem 2004;5:1673–1679. [PubMed: 15532065]
41. Filichev VV, Vester B, Hansen LH, Pedersen EB. Nucleic Acids Res 2005;33:7129–7137. [PubMed: 16377781]
42. Hrdlicka PJ, Kumar TS, Wengel J. Chem. Commun 2005:4279–4281.
43. Kumar TS, Madsen AS, Wengel J, Hrdlicka PJ. J. Org. Chem 2006;71:4188–4201. [PubMed: 16709060]
44. Andersen NK, Wengel J, Hrdlicka PJ. Nucleosides Nucleotides Nucleic Acids 2007;26:1415–1417. [PubMed: 18066795]
45. Kumar TS, Wengel J, Hrdlicka PJ. ChemBioChem 2007;8:1122–1125. [PubMed: 17551917]
46. Kumar TS, Madsen AS, østergaard ME, Wengel J, Hrdlicka PJ. J. Org. Chem 2008;73:7060–7066. [PubMed: 18710289]
47. Kumar TS, Madsen AS, østergaard ME, Sau SP, Wengel J, Hrdlicka PJ. J. Org. Chem 2009;74:1070–1081. [PubMed: 19108636]
48. Mergny JL, Lacroix L. Oligonucleotides 2003;13:515–537. [PubMed: 15025917]
49. Crothers DM. Biopolymers 1968;6:575–584. [PubMed: 5644787]
50. For a representative calculation of ΔG^{293}_{rec} see Table S6†
51. Umemoto T, Hrdlicka PJ, Babu BR, Wengel J. ChemBioChem 2007;8:2240–2248. [PubMed: 17979173]
52. Dioubankova NN, Malakhov AD, Stetsenko DA, Gait MJ, Volynsky PE, Efremov RG, Korshun VA. ChemBioChem 2003;4:841–847. [PubMed: 12964158]
53. Hrdlicka PJ, Babu BR, Sørensen MD, Wengel J. Chem. Commun 2004:1478–1479.
54. Langenegger SM, Häner R. Chem. Commun 2004:2792–2793.
55. Nakamura M, Murakami Y, Sasa K, Hayashi H, Yamana K. J. Am. Chem. Soc 2008;130:6904–6905. [PubMed: 18473465]
56. Winnik FM. Chem. Rev 1993;93:587–614.
57. Reynaldo LP, Vologodskii AV, Neri BP, Lyamichev VI. J. Mol. Biol 2000;297:511–520. [PubMed: 10715217]
58. Kim WJ, Akaike T, Maruyama A. J. Am. Chem. Soc 2002;124:12676–12677. [PubMed: 12392411]
59. Yamana K, Fukunaga Y, Ohtani Y, Sato S, Nakamura M, Kim WJ, Akaike T, Maruyama A. Chem. Commun 2005:2509–2511.
60. Simonson OE, Svahn MG, Törnquist E, Lundin KE, Smith CIE. Curr. Pharmaceut. Design 2005;11:3671–3680.

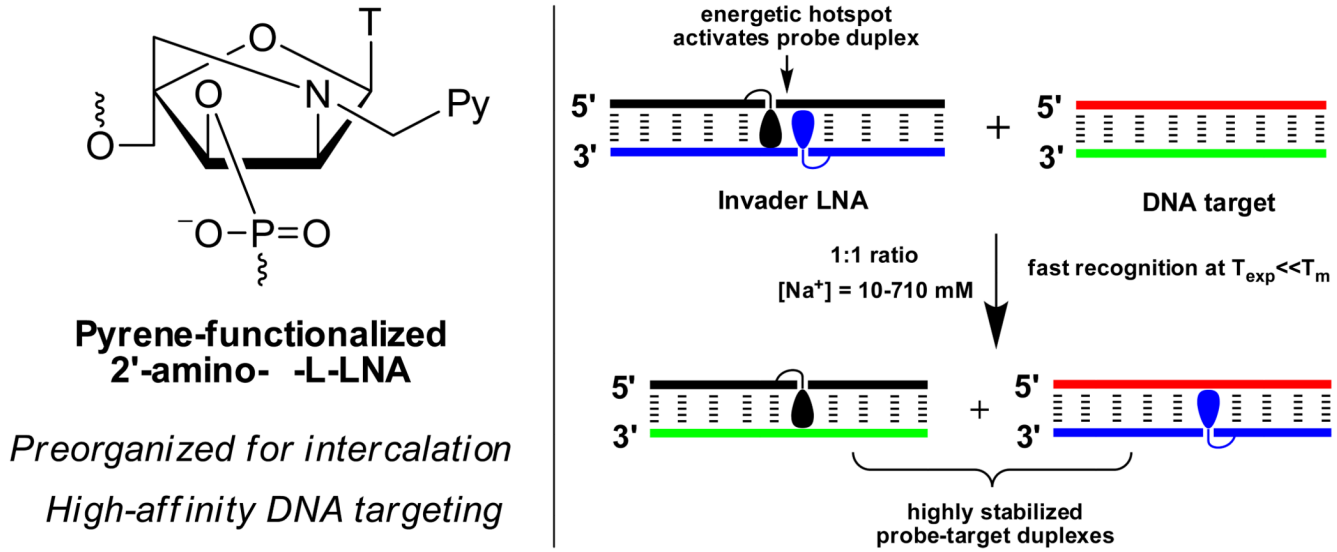

Figure 1.
The Invader LNA concept.

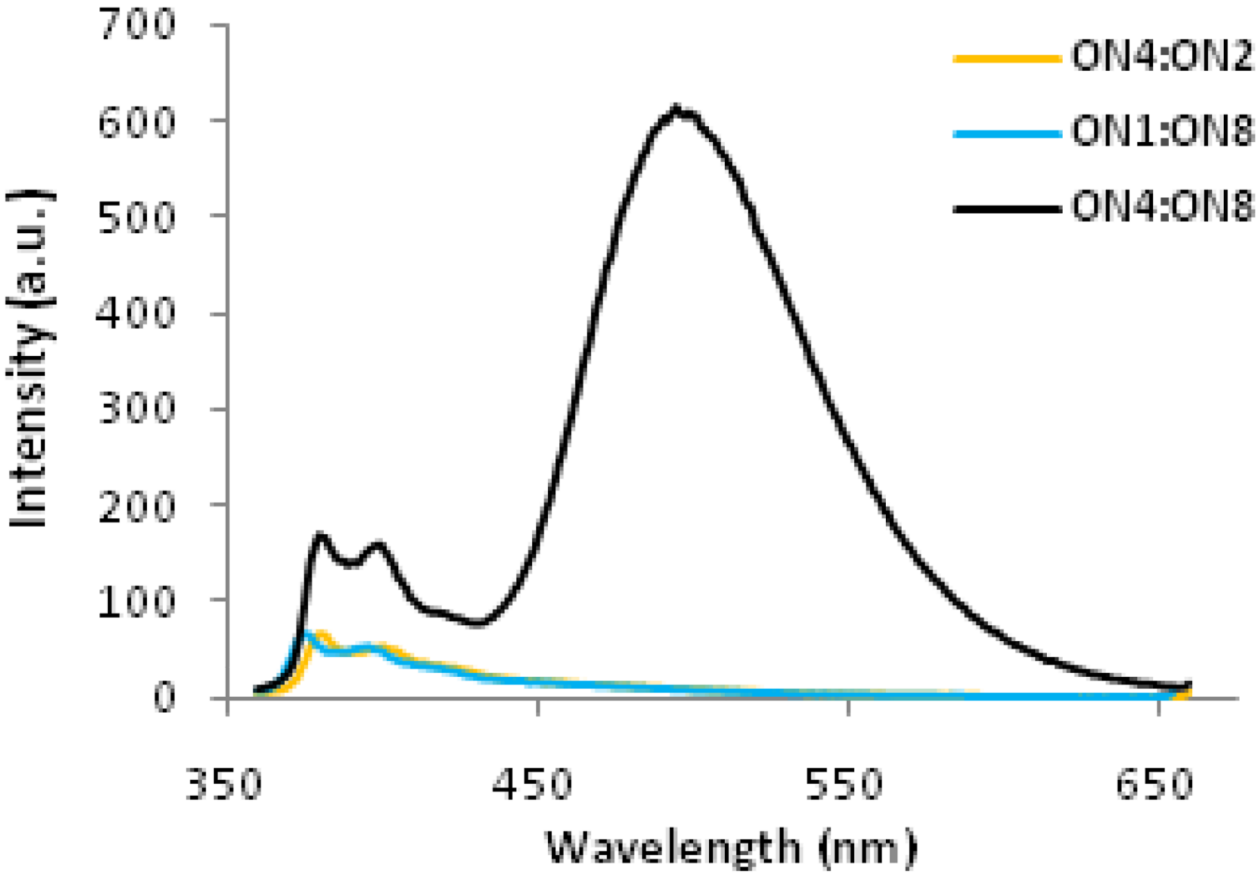

Figure 2.
Steady-state fluorescence emission spectra (λ_{ex} = 335 nm, 20 °C) of Invader LNA probe **ON4**:**ON8** and probe:target duplexes **ON4**:**ON2** and **ON1**:**ON8** recorded in thermal denaturation buffer (all ONs at 1.0 μM concentration). Corresponding spectra for other Invader LNA probes are shown in Fig. S2†.

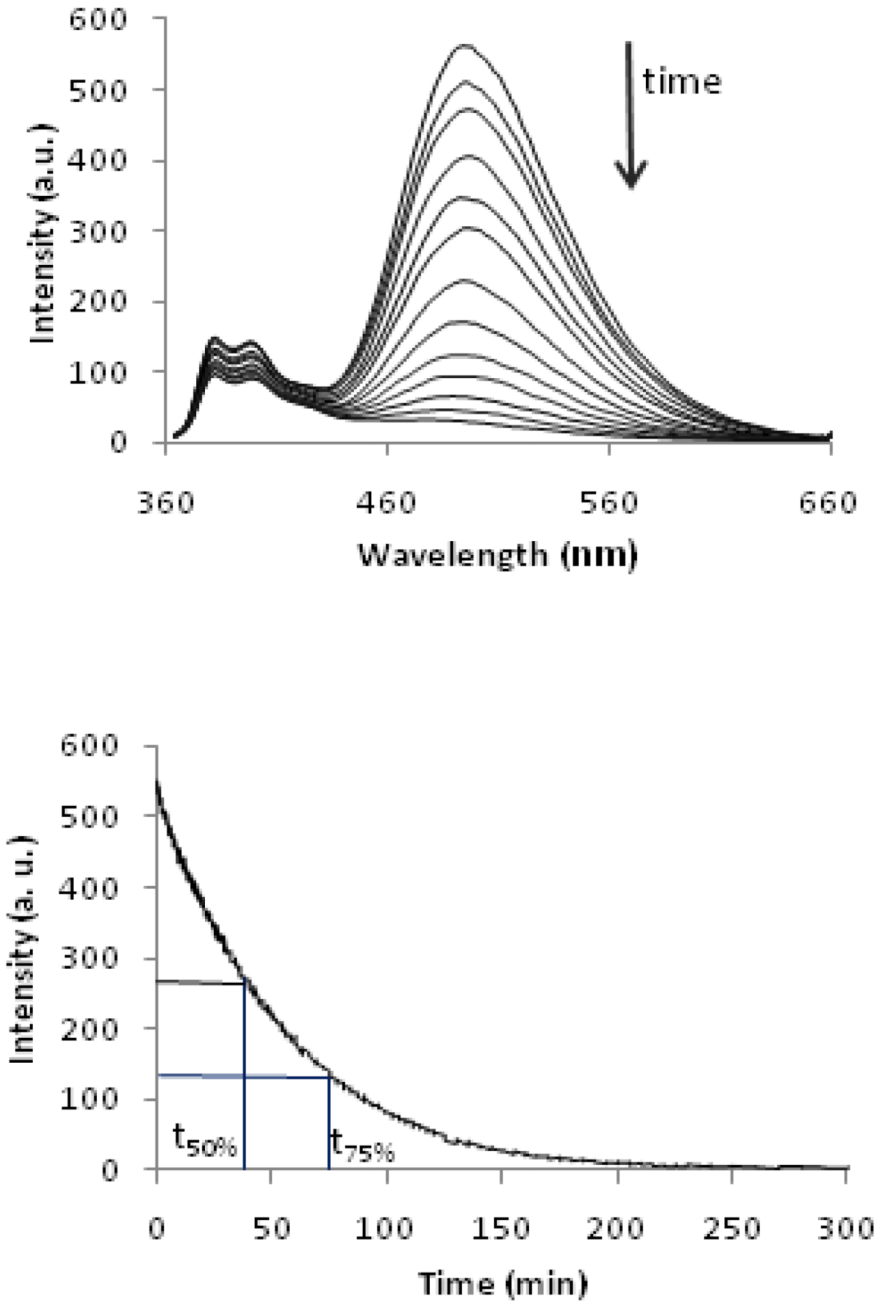

Figure 3.

Upper panel: time course of steady-state fluorescence spectra upon addition of pre-annealed Invader LNA **ON4**:**ON8** to pre-annealed isosequential dsDNA target **ON1**:**ON2** (λ_{ex} = 335 nm, 20 °C, all strands 1.0 μM). Lower panel: time course of fluorescence signal decay at λ_{em} = 495 nm. Corresponding spectra for other Invader LNA are shown in Fig. S3[†].

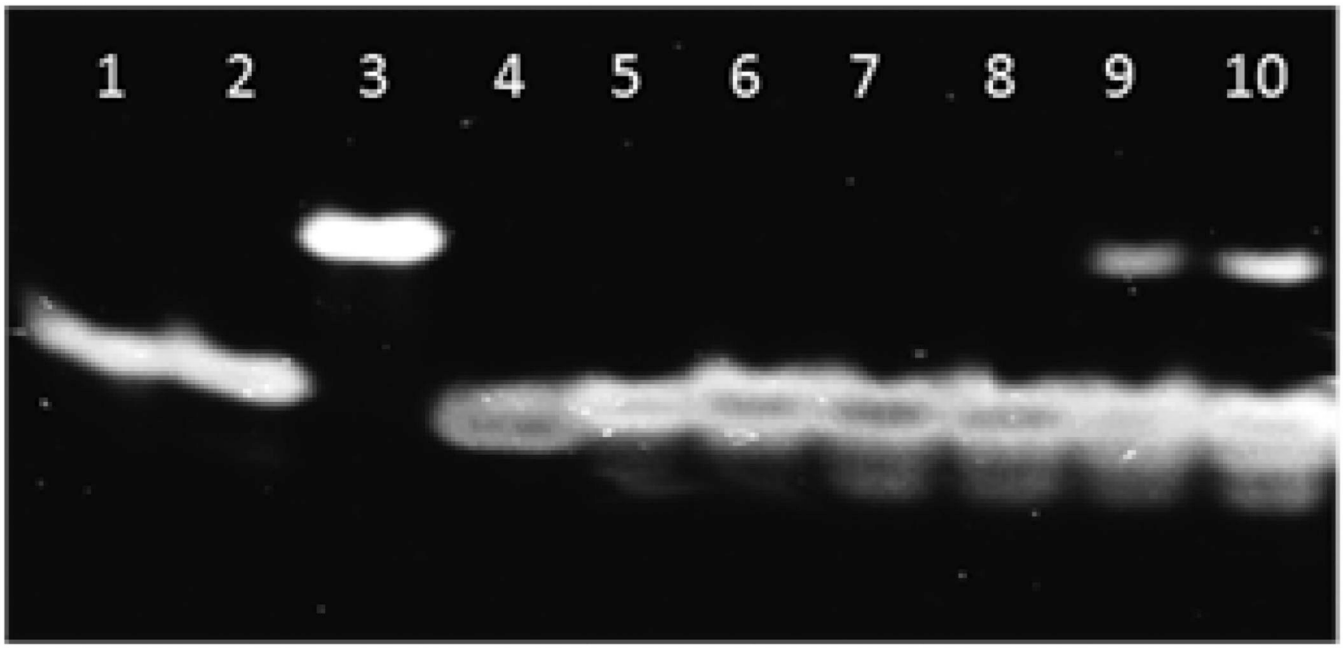

Figure 4.

Electrophoretic mobility shift assay, 16% nondenaturing PAGE run at 4 °C, demonstrating dsDNA-recognition by Invader LNA probes. Probe-target duplex **ON1:ON8** (lane 1); probe-target duplex **ON4:ON2** (lane 2); Invader LNA probe **ON4:ON8** (lane 3); dsDNA target **ON1:ON2** (lane 4); equimolar mixture of Invader LNA probe **ON4:ON8** + dsDNA target **ON1:ON2** which were annealed (lane 5), or incubated at: 37 °C for 4h (lane 6), rt for 4h (lane 7), rt for 8 h (lane 8), 4 °C for 8h (lane 9) or 4 °C for 12h (lane 10), respectively.

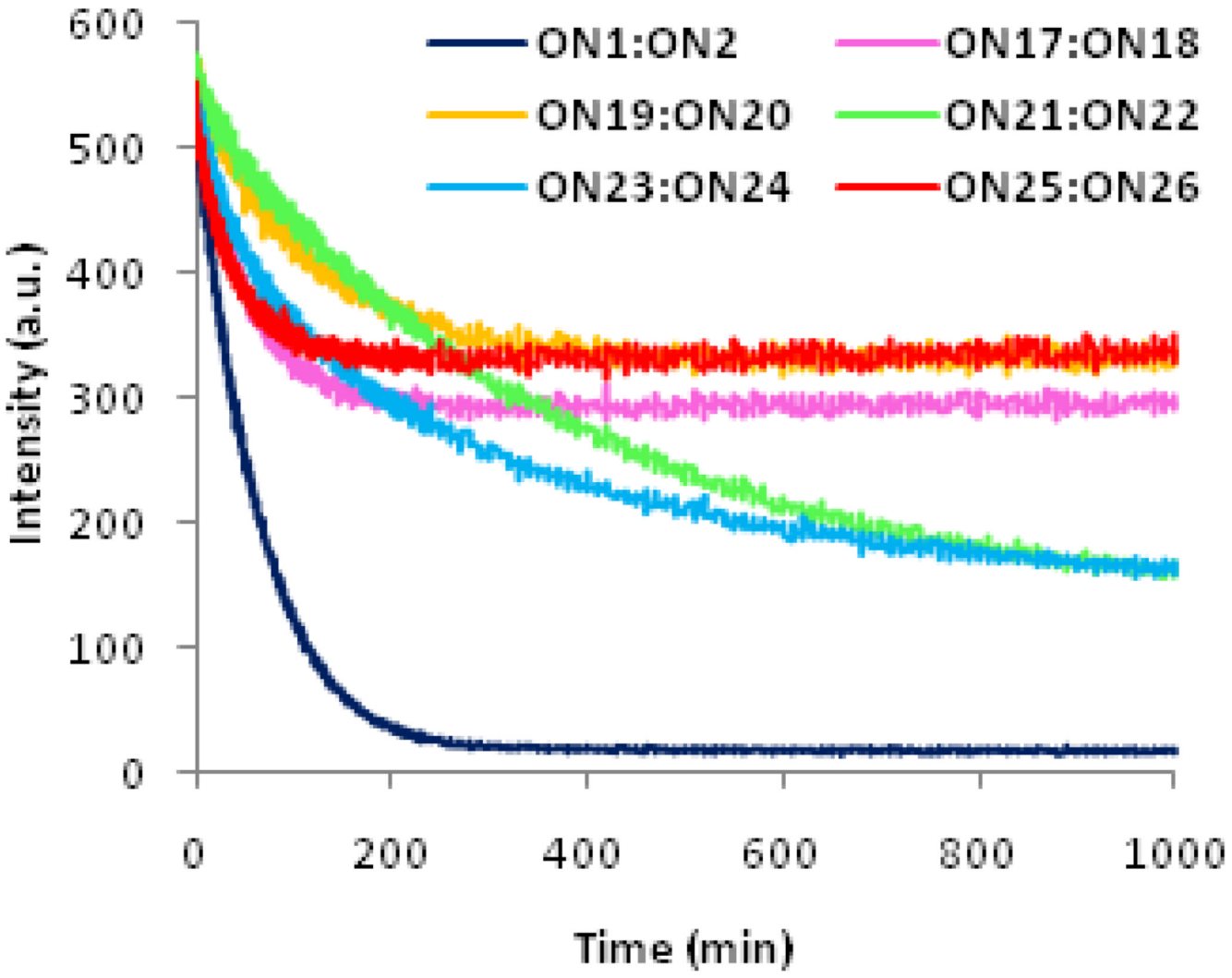

Figure 5.

Time course of fluorescence signal decay at λ_{em} = 495 nm upon addition of pre-annealed Invader LNA **ON4**:**ON8** to pre-annealed isosequential dsDNA **ON1**:**ON2** or fully base paired non-isosequential dsDNA targets. Sequences of targets **ON17**–**ON26** are shown in Table 4. Conditions are as described in Figure 2.

Table 1

Hybridization data for duplexes between 2'-*N*-(pyren-1-yl)methyl-2'-amino-α-L-LNA **ON3–ON16** and complementary DNA.[a]

Entry	ON	Duplex	T_m [ΔT_m] (°C)	ΔH [$\Delta\Delta H$] (kJ/mol)	($T_{293}\Delta S$) [$\Delta(T_{293}\Delta S)$] (kJ/mol)	ΔG_{293} [$\Delta\Delta G_{293}$] (kJ/mol)
1	**ON1**	5'-d(GGT ATA TAT AGG C)	37.5	−382	−325	−57
	ON2	3'-d(CCA TAT ATA TCC G)	-	-	-	-
2	**ON3**	5'-d(GG**X** ATA TAT AGG C)	44.5	−316	−256	−60
	ON2	3'-d(CCA TAT ATA TCC G)	[+7.0]	[+66]	[+69]	[−3]
3	**ON4**	5'-d(GGT A**X**A TAT AGG C)	47.5	−356	−290	−66
	ON2	3'-d(CCA TAT ATA TCC G)	[+10.0]	[+26]	[+35]	[−9]
4	**ON5**	5'-d(GGT ATA **X**AT AGG C)	49.0	−380	−311	−69
	ON2	3'-d(CCA TAT ATA TCC G)	[+11.5]	[+2]	[+14]	[−12]
5	**ON6**	5'-d(GGT ATA TA**X** AGG C)	47.0	−358	−293	−66
	ON2	3'-d(CCA TAT ATA TCC G)	[+9.5]	[+24]	[+32]	[−9]
6	**ON1**	5'-d(GGT ATA TAT AGG C)	48.5	−409	−338	−71
	ON7	3'-d(CCA **X**AT ATA TCC G)	[+11.0]	[−27]	[−13]	[−14]
7	**ON1**	5'-d(GGT ATA TAT AGG C)	48.5	−383	−314	−70
	ON8	3'-d(CCA TA**X** ATA TCC G)	[+11.0]	[−1]	[+11]	[−13]
8	**ON1**	5'-d(GGT ATA TAT AGG C)	48.0	−390	−320	−70
	ON9	3'-d(CCA TAT A**X**A TCC G)	[+10.5]	[−8]	[+5]	[−13]
9	**ON1**	5'-d(GGT ATA TAT AGG C)	47.0	−392	−325	−67
	ON10	3'-d(CCA TAT ATA **X**CC G)	[+9.5]	[−10]	[0]	[−10]
10	**ON11**	5'-d(GG**X** A**X**A TAT AGG C)	53.5	−300	−233	−66
	ON2	3'-d(CCA TAT ATA TCC G)	[+16.0]	[+82]	[+92]	[−9]
11	**ON12**	5'-d(GG**X** ATA **X**AT AGG C)	57.5	−340	−266	−74
	ON2	3'-d(CCA TAT ATA TCC G)	[+20.0]	[+42]	[+59]	[−17]
12	**ON13**	5'-d(GG**X** ATA TA**X** AGG C)	56.5	−399	−319	−80
	ON2	3'-d(CCA TAT ATA TCC G)	[+19.0]	[−17]	[+6]	[−23]
13	**ON1**	5'-d(GGT ATA TAT AGG C)	57.5	−385	−306	−79
	ON14	3'-d(CCA **X**A**X** ATA TCC G)	[+20.0]	[−3]	[+19]	[−22]
14	**ON1**	5'-d(GGT ATA TAT AGG C)	61.0	−414	−328	−86

Entry	ON	Duplex	T_m [ΔT_m] (°C)	ΔH [$\Delta\Delta H$] (kJ/mol)	($T_{293}\Delta S$) [$\Delta(T_{293}\Delta S)$] (kJ/mol)	ΔG_{293} [$\Delta\Delta G_{293}$] (kJ/mol)
15	**ON15**	3'-d(CCA **X**AT A**X**A TCC G)	[+23.5]	[−32]	[−3]	[−29]
	ON1	5'-d(GGT ATA TAT AGG C)	59.0	−405	−322	−83
	ON16	3'-d(CCA **X**AT ATA **X**CC G)	[+21.5]	[−23]	[+3]	[−26]

[a] T_m-values (ΔT_m = change in T_m-value relative to **ON1**:**ON2**) and Gibbs free energy of duplex formation at 293 K, ΔG^{293}, determined by baseline fitting of optical melting curve (A_{260} vs T) recorded in medium salt buffer ([Na^+] = 110 mM, [Cl-] = 100 mM, pH 7.0 (adjusted with NaH_2PO_4/Na_2HPO_4)), using 1.0 μM of each strand. Values are averages of at least two measurements. $\Delta\Delta G^{293}$ = difference in Gibbs free energy of duplex formation relative to reference duplex **ON1**:**ON2**. For structure of monomer **X**, see Fig. 1.

Table 2

Hybridization data for Invader LNA probes and their free energy, ΔG^{293}_{rec}, for recognition of dsDNA target **ON1**:**ON2** at 293 K.[a]

Entry	ON	Duplex	T_m [ΔT_m] (°C)	ΔH[$\Delta\Delta H$] (kJ/mol)	($T^{293}\Delta S$)[$\Delta(T^{293}\Delta S)$] (kJ/mol)	ΔG^{293}[$\Delta\Delta G^{293}$] (kJ/mol)	ΔG^{293}_{rec} (kJ/mol)
1	**ON3**	5’-d(GG**X** ATA TAT AGG C)	36.5	−262	−214	−48	−26
	ON7	3’-d(CCA **X**AT ATA TCC G)	[−1.0]	[+120]	[+111]	[+9]	
2	**ON4**	5’-d(GGT A**X**A TAT AGG C)	41.0	−360	−301	−60	−19
	ON8	3’-d(CCA TA**X** ATA TCC G)	[+3.5]	[+22]	[+24]	[−3]	
3	**ON5**	5’-d(GGT ATA **X**AT AGG C)	40.5	−375	−315	−60	−22
	ON9	3’-d(CCA TAT A**X**A TCC G)	[+3.0]	[+7]	[+10]	[−3]	
4	**ON6**	5’-d(GGT ATA TA**X** AGG C)	36.0	−311	−260	−51	−24
	ON10	3’-d(CCA TAT ATA **X**CC G)	[−1.5]	[+71]	[+65]	[+6]	
5	**ON11**	5’-d(GG**X** A**X**A TAT AGG C)	48.0	−219	−165	−55	−34
	ON14	3’-d(CCA **X**A**X** ATA TCC G)	[+10.5]	[+163]	[+160]	[+2]	
6	**ON12**	5’-d(GG**X** ATA **X**AT AGG C)	53.0	−209	−152	−56	−47
	ON15	3’-d(CCA **X**AT A**X**A TCC G)	[+15.5]	[+173]	[+173]	[+1]	
7	**ON13**	5’-d(GG**X** ATA TA**X** AGG C)	48.0	−230	−175	−55	−50
	ON16	3’-d(CCA **X**AT ATA **X**CC G)	[+10.5]	[+152]	[+150]	[+2]	

[a] Conditions as specified in Table 1.

Table 3

Kinetic parameters ($t_{50\%}/t_{75\%}$ [min]) for recognition of isosequential dsDNA-target ON1:ON2 by selected Invader LNA.[a]

Buffer	ON4:ON8		ON6:ON10		ON11:ON14		ON13:ON16	
	$t_{50\%}$	$t_{75\%}$	$t_{50\%}$	$t_{75\%}$	$t_{50\%}$	$t_{75\%}$	$t_{50\%}$	$t_{75\%}$
MS	38	74	34	67	29	60	48	103
HS	126	257	-	-	31	68	-	-
KMST	158	296	-	-	19	42	-	-

[a][probe] = [target] = 1.0 μM; $t_{50\%}$ and $t_{75\%}$ = time in min required to reduce fluorescence intensity at λ_{em} = 495 nm by 50% and 75%, respectively. MS = medium salt, HS = high salt, KMST-buffer specified in main text

Table 4

Hybridization data for non-isosequential dsDNA targets and the available free energy, ΔG^{293}_{rec} for their recognition by Invader LNA probe **ON4**:**ON8** at 293 K.[a]

ON	Duplex	T_m (°C)	ΔG^{293} (kJ/mol)	ΔG^{293}_{rec} (kJ/mol)
ON1	5’-d(GGT ATA TAT AGG C)	37.5	−57	−26
ON2	3’-d(CCA TAT ATA TCC G)			
ON17	5’-d(GGA ATA TAT AGG C)	38.5	−59	+8
ON18	3’-d(CCT TAT ATA TCC G)			
ON19	5’-d(GGT ATC TAT AGG C)	41.0	−60	+6
ON20	3’-d(CCA TAG ATA TCC G)			
ON21	5’-d(GGT ATG TAT AGG C)	42.0	−60	−1
ON22	3’-d(CCA TAC ATA TCC G)			
ON23	5’-d(GGT ATT TAT AGG C)	38.5	−57	0
ON24	3’-d(CCA TAA ATA TCC G)			
ON25	5’-d(GGT ATA TAA AGG C)	38.0	−58	+7
ON26	3’-d(CCA TAT ATT TCC G)			

[a] Conditions as specified in Table 1. Underlined positions denote sites of sequence disparity relative to Invader LNA **ON4**:**ON8**.

Table 5

Hybridization data for duplexes involving **ON4** or **ON8** and mismatched DNA.[a]

Entry	ON	Sequence	T_m [ΔT_m] (°C)	ΔG_{293} [$\Delta(\Delta G_{293})$] (kJ/mol)
1	**ON17**	5’-d(GGA ATA TAT AGG C)	39.5	−57
	ON8	3’-d(CCA TA**X** ATA TCC G)	[−9.0]	[+13]
2	**ON19**	5’-d(GGT ATC TAT AGG C)	39.0	−58
	ON8	3’-d(CCA TA**X** ATA TCC G)	[−9.5]	[+12]
3	**ON21**	5’-d(GGT ATG TAT AGG C)	44.5	−63
	ON8	3’-d(CCA TA**X** ATA TCC G)	[−4.0]	[+7]
4	**ON23**	5’-d(GGT ATT TAT AGG C)	46.0	−64
	ON8	3’-d(CCA TA**X** ATA TCC G)	[−2.5]	[+6]
5	**ON25**	5’-d(GGT ATA TAA AGG C)	37.0	−55
	ON8	3’-d(CCA TA**X** ATA TCC G)	[−11.5]	[+15]
6	**ON4**	5’-d(GGT A**X**A TAT AGG C)	37.5	−54
	ON18	3’-d(CCT TAT ATA TCC G)	[−10.0]	[+12]
7	**ON4**	5’-d(GGT A**X**A TAT AGG C)	38.0	−56
	ON20	3’-d(CCA TAG ATA TCC G)	[−9.5]	[+10]
8	**ON4**	5’-d(GGT A**X** A TAT AGG C)	39.5	−58
	ON22	3’-d(CCA TAC ATA TCC G)	[−8.0]	[+8]
9	**ON4**	5’-d(GGT A**X** A TAT AGG C)	35.0	−53
	ON24	3’-d(CCA TAA ATA TCC G)	[−12.5]	[+13]
10	**ON4**	5’-d(GGT A**X**A TAT AGG C)	38.0	−56
	ON26	3’-d(CCA TAT ATT TCC G)	[−9.5]	[+10]

[a] Conditions as specified in Table 1. Underlined positions denote position of mismatched base pairs. ΔT_m = change in T_m value and $\Delta(\Delta G^{293})$ = difference in ΔG^{293} value, relative to fully matched **ON1**:**ON8** (entries 1–5) or **ON4**:**ON2** (entries 6–10).